Int. J. Advanced Design and Manufacturing Technology, 2022, Vol. 15, No. 4, pp. 47-60

DOI: 10.30486/ADMT.2022.1957347.1348 ISSN: 2252-0406 https://admt.isfahan.iau.ir

Numerical Investigation of Forced Convection Heat Transfer for Different Models of PPFHS Heatsinks

Soheil Sadrabadi Haghighi, Hamid Reza Goshayeshi *, Iman Zahmatkesh

Department of Mechanical Engineering,
Mashhad Branch, Islamic Azad University, Mashhad, Iran
E-mail: soheilsadrabadi@gmail.com, goshayshi@yahoo.com, Zahmatkesh55310@mshdiau.ac.ir
*Corresponding author

Received: 24 April 2022, Revised: 13 September 2022, Accepted: 17 September 2022

Abstract: In his research article, several models of heatsink were optimally designed in fin length, width and height along with pin placement which consists of 4 pin fin heatsink models heatsink (including square with different pin angles, circular, truncated cone, and cone pin heatsinks and one model of the plate-fin heatsink (PFHS)) in order to achieve better thermal performance as well as less energy consumption and were numerically investigated under high air velocity and heat fluxes. Different parameters such as peak temperature, Nusselt number, heat resistance, pressure drop, and energy consumption were compared. The results show that the square PPFHS with the pin angle of 45 degrees has the highest thermal performance compared to the rest of the models while also having the highest pressure drop and energy consumption between the models consuming more than 255 and 358 percent more energy in order to have the same air velocity in the pathway, while the truncated and the fully formed cone model despite having 25% and 30% less thermal performance, have the least pressure drop between the pin models of the heatsinks and therefore consume the least energy out of the PPFHS.

Keywords: Energy Consumption, Nusselt Number, Thermal Resistance, Thermal Performance, Truncated Cone

Biographical notes: Soheil Sadrabadi Haghighi received his BSc and MSc in Mechanical Engineering from the Islamic Azad University in Mashhad in 2016. He is currently a PhD student in Islamic Azad University, Mashhad Branch. His current research interests include improving pool boiling heat transfer by nanoparticles and computational fluid dynamics (CFD) and optimization of energy systems. **Hamid Reza Goshayeshi** received his PhD from South Bank University in London, England in 1999, and did his post-doctoral research on the same university in 2003. His current research interest includes solar still, nanofluid, heat sink, boiling heat transfer and other heat transfer enchantments methods. **Iman Zahmatkesh** is Associate Professor of Mechanical Engineering at Islamic Azad University, Mashhad Branch. He received his PhD in the Mechanical Engineering from Shiraz University, Iran in 2011.

Research paper

1 INTRODUCTION

Heat transfer is one of the most important concepts which is used in chemical engineering and mechanical engineering and other fields [1-2]. This includes wide applications such as electronic systems, robotics, MEMS, and housing temperature regulation. There are various methods of cooling available which include heat exchangers, heat pipes, water cooling, and more [3-5]. One of the most important pieces of cooling equipment used today is the heats sink. The most important feature of a heatsink is heat dissipation and cooling. A heatsink is a piece of metal with a high thermal conductivity that is mounted on electrical or electronic components and captures the heat and heat generated by the part, then through heat exchange with the surrounding environment and cooling with air (in some models Water) reduces heat [6-9]. This part is even used in various voltage converters or car inverters and audio and video. There are two methods of cooling solution and heat generation management for heatsinks which are active cooling and passive cooling. In passive type heatsink, the temperature control operation is performed by convection process, which is one of the concepts of heat transfer science [10]. In this way, the passive heatsink absorbs heat from the desired part and distributes the heat in that fluid by maximizing the contact surface with the surrounding fluid through the fins (blades). The absence of moving parts has increased the reliability of this type of heatsink. Of course, it is important to realize the fact that in order to transfer heat in passive heatsinks, a constant flow of air must be constantly passing through the fans [11-14]. One of the most important aspects of the heat sink that must be considered in its design is a simpler structure, high heat transfer rate, and low-pressure drop.

Liquid cooling methods can dissipate more heat at smaller footprints. However, they have the disadvantage of complexity of design, expense, and require maintenance regularly [15]. In active cooling, a fan or blower is usually used as the heat transfer element. This type of heatsink has very high efficiency. Of course, due to the higher price, it is less used than the passive type [16]. Extended surfaces used in cooling systems, which are commonly named fins, are utilized across all electronic application as arrays or heat sinks name. Generated heat transfers to the heat sinks by conduction heat transfer, and the transported heat dissipates through the environment around it via convection heat transfer [17]. Kim et al. [18] compared and evaluated the thermal characteristics of plate-fin and plate pin-fin heat sinks experimentally. Both of these models were subjected to a parallel airflow. They have discovered that there is a correlation between Nusselt number and the friction coefficient factor for both models of heat sinks. They also discovered that pumping power and length of the heat sink are important factors that affects heatsinks thermal performance. Ambreen & Kim [19] numerically experimented on and investigated the thermal characteristics of a square cylinder under a laminar flow. Scholten et al. [20] developed an empirical model in order to study the heat flow and heat transfer rate of a cylinder. This model also allowed them to study the velocity and velocity profile under a transverse flow. A. Bhattacharyya et al. [21] have performed numerical studies in order to predict the thermal behaviour of hexagonal cylinder under a cross-flow. They have discovered that both Nusselt number as well as Reynolds number have a significant effect on the intensity of the turbulence flow as well as the pressure coefficient in the flow regime. Benim et al. [22] investigated fluid passing around a circular cylinder. In this experiments they proposed several turbulence modelling strategy in order to simulate an incompressible turbulent fluid passing around the circular cylinder. Kitti et al [23] discovered that in plate pin heat sinks, pin fin configuration is an important parameter and has significant effects on thermal performance and airflow characteristic. They also discovered that changing fin characteristics such as fin shape, pin fin orientation, and the ratio of the distance between pin and plate-fin centre to pin fin size affects thermal performance, heat transfer coefficient and pressure drop.

Nilpueng & Wongwises [24] investigated the twist ratio and perforation diameter and its influence on a model of PFHS with twisted tape. The results show that lowering the twist ration with the same perforation diameter has a positive effect on the enhancement ratio. Ahmet et al. [25] experimentally discovered that pin geometry such as height and other factors such as pin spacing and orientation is vital for better thermal performance in natural convection heat transfer. This experiment was performed with inline pin fin and plate heat sinks. They also discovered that the upward-facing orientation of 0° orientation angle has the highest heat transfer, while the lowest heat transfer rate was for the heat sink with the downward-facing 180° orientation angle. Emad et al. [26] experimented the thermo-hydraulic performance by changing the twist angle on a heat sink with square and hexagonal pin fin array under forced convection heat transfer. They discovered that by twisting the fins the thermal resistance decreases when compared to the non-twisted pins. They have also concluded that increasing the twisting angle lowers the friction factor and pressure drop while also lowering the efficiency when compared to no twisted fins. Singh et al. [27] investigated the heat transfer and thermal-hydraulic performance of a heat sink with square micro pin fins under forced convection heat transfer. The results show that by increasing the fin height, thermal resistance decreases while pressure drop increases. Thermal performance and heat coefficient increase with the increase of fin height and Reynolds

number but it decreases with increasing fin spacing. The percentage of improvement in efficiency was observed to be about 2 to 9% due to the presence of fins on the impingement surface, flow mixing, disruption of the boundary layers, and augmentation of turbulent transport. Dnyaneshwar & Vithoba [28] investigated pin fin arrangement effectiveness on heat sink heat transfer characteristics. Davoudi et al. [29] numerically investigated the effects of using nanofluid on heat transfer in a conical spiral heat exchanger. The nanofluids used in this numerical simulation were aluminum oxide/water (Al2O3/water) and copper oxide/water (CuO/water). They have discovered from the results that enhancing the concentration of the nanofluid causes the pressure drop to increase and heat transfer rate is slightly increased by adding nanoparticles to the base water fluid in very low concentration. They also discovered that vortices formed at the top and bottom of the tube slightly increases by enhancing the concentration of nanofluids and this flow produces more power.

While there are many different forms of heatsinks with different fin and pin arrangements, most models used are usually plate fin based heatsink or have circular pin fin arrangement. Rarely heatsink uses square shape, truncated cone or cone shaped pin in their designs. In this research, several new models of heatsinks are designed with the focus on different fin geometry and arrangement. These pin-fin based heatsink models consist of a plate fin heatsink and several other models of pin fin based heatsinks which were optimized in length, width, height and fin arrangement in order to produce optimized results and achieve better thermal performance and as well as to reach lover energy consumption. Most studies on heatsinks also tend focus on lower Reynolds numbers. In this research higher Reynolds number and therefore higher air velocity are considered for this study in order to study the effects of such high air velocity on thermal performance, pressure drop, energy consumption and Nusselt numbers. The purpose of this research is to numerically investigate these heatsink models in order to find out with models is suited for higher air velocity as well as compare thermal performance and energy consumption in height and relatively low Reynolds number.

2 MODEL DESIGN

The shape and geometric parameters of this model are based on the model of Yu et al. [30]. The types of heatsinks are shown in "Figs. 1 to 8" and the properties are shown in Table 1. These models were numerically tested. The distance between the pins and the fin is measured to be at least 1D and the distance between the pins is 10D. These models include the PFHS model, and PPFHS models with a circle, truncated, cone, and square pins. The Square PPFHS pins have three arrangements with the angles of 0,22.5, and 45 degrees which are shown in "Figs. 4, 7, and 8". The computer model in this experiment is based on the model of Yu et al. [30], which is shown in "Fig 9".

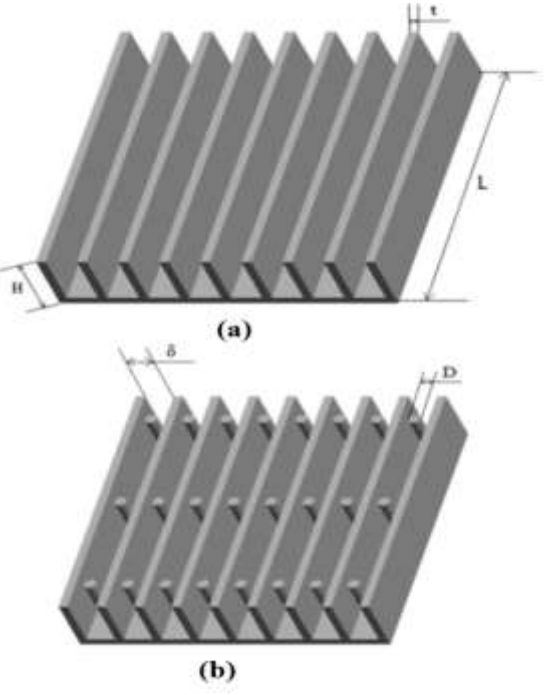

Fig. 1 Heatsink model dimensions: (a): plate pin fin heatsink, and (b): circular pin fin heatsink.

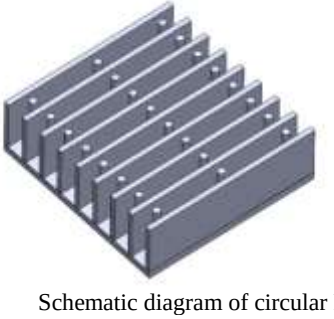

Fig. 2 Schematic diagram of circular PPFHS.

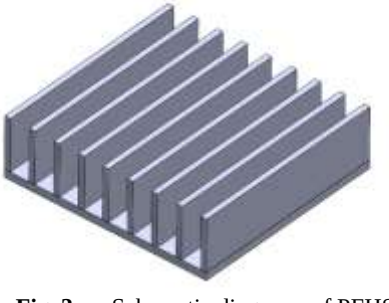

Fig. 3 Schematic diagrams of PFHS.

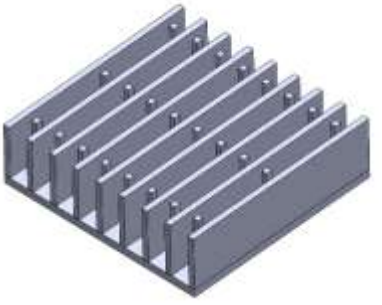

Fig. 4 Schematic diagram of square PPFHS.

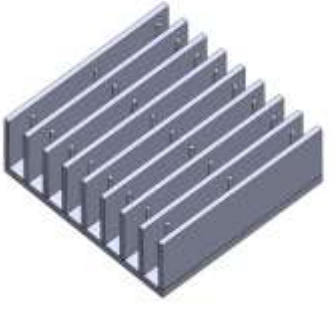

Fig. 5 Schematic diagram of truncated cone PPFHS.

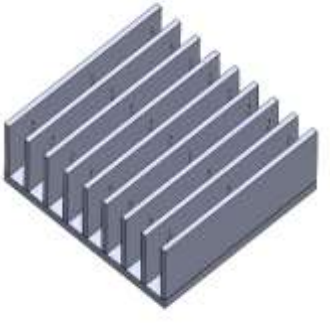

Fig. 6 Schematic diagram of cone PPFHS.

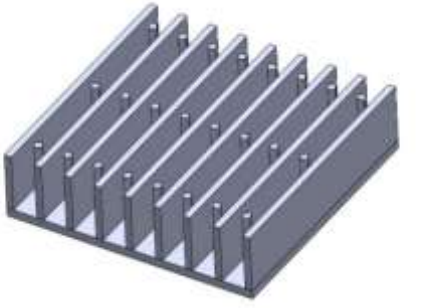

Fig. 7 Schematic diagram of square PPFHS with pin angle of 22.5 degrees.

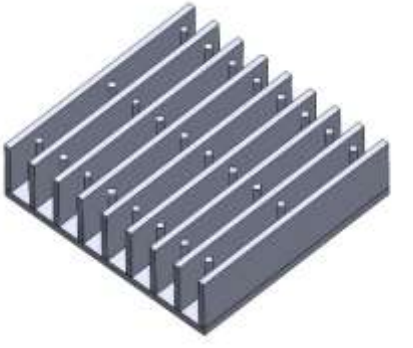

Fig. 8 Schematic diagram of square PPFHS with pin angle of 45 degrees.

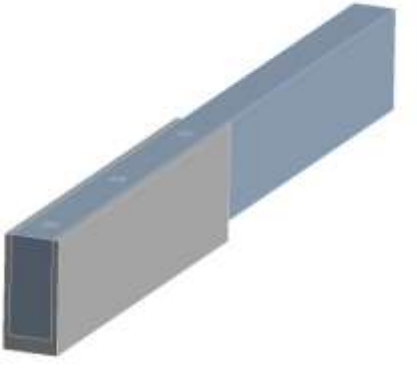

Fig. 9 Computer model of square PPFHS

Table 1 Types of heatsink under numerical experiment

Type of Heat sink	Type of Pin	Base Diameter (D)	End Diameter	Fin spacing	Fin Height (H)	Fin Thickness (δ)	Angle of pin
PFHS	N/A	N/A	N/A	5mm	10mm	1.5mm	N/A
PPFHS	Circular	2mm	2mm	5mm	10mm	1.5mm	N/A
PPFHS	Square	2mm	2mm	5mm	10mm	1.5mm	0
PPFHS	Truncated Cone	2mm	1mm	5mm	10mm	1.5mm	N/A
PPFHS	Cone	2mm	0.1mm	5mm	10mm	1.5mm	N/A
PPFHS	Square	2mm	2mm	5mm	10mm	1.5mm	22.5
PPFHS	Square	2mm	2mm	5mm	10mm	1.5mm	45

3 MATHEMATICAL EQUATION OF HEAT SINK MODEL AND NUMERICAL SIMULATION

As shown in the geometric model, both region of the heat sink model (fluid and solid) participates in the numerical simulation of heat sink models. For this numerical simulation, the k-epsilon turbulent model is used to simulate the turbulent fluid flow in the heat sink passage. The mathematical Equation governing this are as follows:

The dimensionless continuity, momentum, and energy Equation can be written as:

$$\frac{\delta U}{\partial X}+\frac{\delta V}{\partial Y}+\frac{\delta W}{\partial Z}=0 \tag{1}$$

$$U\frac{\partial U}{\partial X}+V\frac{\partial U}{\partial Y}+W\frac{\partial U}{\partial Z}=-\frac{dP}{dX}+\frac{1}{\mathrm{Re}}(\frac{\partial^2 U}{\partial X^2}+\frac{\partial^2 U}{\partial Y^2}+\frac{\partial^2 U}{\partial Z^2}) \tag{2}$$

$$U\frac{\partial V}{\partial X}+V\frac{\partial V}{\partial Y}+W\frac{\partial V}{\partial Z}=-\frac{dP}{dY}+\frac{1}{\mathrm{Re}}(\frac{\partial^2 V}{\partial X^2}+\frac{\partial^2 V}{\partial Y^2}+\frac{\partial^2 V}{\partial Z^2}) \tag{3}$$

$$U\frac{\partial W}{\partial X}+V\frac{\partial W}{\partial Y}+W\frac{\partial W}{\partial Z}=-\frac{dP}{dY}+\frac{1}{\mathrm{Re}}(\frac{\partial^2 W}{\partial X^2}+\frac{\partial^2 W}{\partial Y^2}+\frac{\partial^2 W}{\partial Z^2}) \tag{4}$$

$$U\frac{\partial \theta}{\partial X}+V\frac{\partial \theta}{\partial Y}+W\frac{\partial \theta}{\partial Z}=\frac{1}{\mathrm{Re.Pr}}(\frac{\partial^2 \theta}{\partial X^2}+\frac{\partial^2 \theta}{\partial Y^2}+\frac{\partial^2 \theta}{\partial Z^2}) \tag{5}$$

For the solid part of the thermal heatsink, the energy Equation is as follows:

$$\frac{\partial^2 \theta}{\partial X^2}=0 \tag{6}$$

The dimensionless parameters in the previous Equations can be found as:

$$X=\frac{x}{Dh},\frac{y}{Dh},Z=\frac{z}{Dh},U=\frac{u}{u_{in}},V=\frac{v}{u_{in}},$$
$$P=\frac{p}{\rho u_{in}},W=\frac{w}{u_{in}},\theta=\frac{T_f-T_{in}}{T_w-T_{in}}$$

The pressure difference is obtained from the following relation:

$$\Delta p=p_{in}-p_{out} \tag{7}$$

Heat sink heat resistance can be defined as follows [31]:

$$R_{th}=\frac{\Delta T}{Q} \tag{8}$$

ΔT is the temperature difference between the fin base and ambient air temperature, while Q shows the thermal power pumped to base of the heatsink fin. This Equation is used to measure the thermal performance of the heat sink models. In order to find the power needed to support the heat flux, the heat sink can be found via Sparrow and Ramsey [32] Equation:

$$E=U_{in}A_p\Delta p \tag{9}$$

$$A_p=H\delta(N-1) \tag{10}$$

Reynold's number can be calculated using this Equation:

$$\mathrm{Re}=\frac{\rho V D_H}{\mu} \tag{11}$$

And the Nusselt number can be calculated from:

$$Nu=\frac{hD_h}{k} \tag{12}$$

The downstream boundary is located at a distance L from the edge of the fin in the x direction to prevent backflow. In this simulation, the input and output boundary conditions of the pressure are assumed to be uniform. The two side walls are symmetrically adjusted using the periodic structure assumption. It is assumed that all enclosed walls, except the heating zone, have non-slip condition and are adiabatic. Furthermore, to simulate the heat transfer between the fin and base surfaces, the fluid is characterized as a wall-coupled condition, through which the process is performed automatically without external interference. The output of the model is pressure outlet and can be seen in "Fig. 9". The air current inlet is uniform with the velocity of 6,8,10, and 12 m/s with constant flux conditions of 0.5,1.5, and 2.5 watts per square centimetre. The ambient temperature is 294 kelvins.

General computational fluid dynamics software has been selected for the heat sink model simulation. It is an advanced CFD software which offers many different turbulence models. The software uses a semi-implicit method for the pressure-related Equation algorithm (SIMPLE) based on a volume control program using a pressure-based solver. The Equation used to solve the turbulent flow of the k-epsilon method and the remainder for the continuity, momentum, energy, and k and epsilon Equations are less than 10^{-3}, 10^{-5}, 10^{-6}, 10^{-3}, 10^{-3}.

4 VALIDATION AND REVIEW OF RESULTS

In order to validate the model, the laboratory and numerical model of Yu et al. [33] has been used, which can be seen in "Fig. 10 and Fig. 11". Examination of these two shows that the result obtained is an acceptable value. For the Grid independence test for each of these models, the minimum of 234990 nodes was used in creating a triangular mesh model and the results showed that the properties change was less than 1 percent for the thermal performance when we increased the mesh from that number.

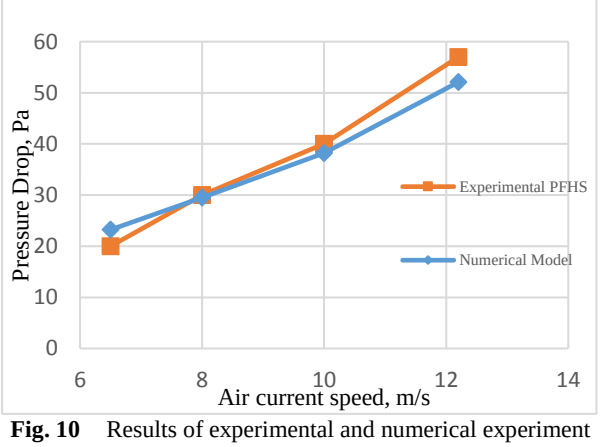

Fig. 10 Results of experimental and numerical experiment of PFHS models.

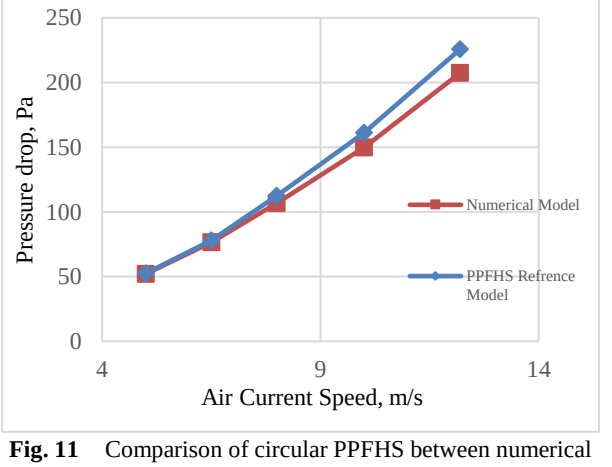

Fig. 11 Comparison of circular PPFHS between numerical and reference model.

5 RESULTS AND DISCUSSION

In this experiment, 7 models of heatsinks were compared under different velocity inputs and different heat fluxes. The peak temperatures of these different models are shown in "Figs. 12, 13, and 14" for each heat flux respectively. These figures show that the heat sink with angled square pins has the lowest peak temperature when compared to the rest of the models. The circular pin and square pin heatsink with 0 degrees' deflection angle has nearly the same peak temperature with the highest difference of fewer than 2 degrees Kelvin. The truncated cone pin heat sink is the next coldest heat sink, Because of its geometry and having less cross-area with air compared to the circular and square pin heatsink. This is the same for the cone pin heatsink.

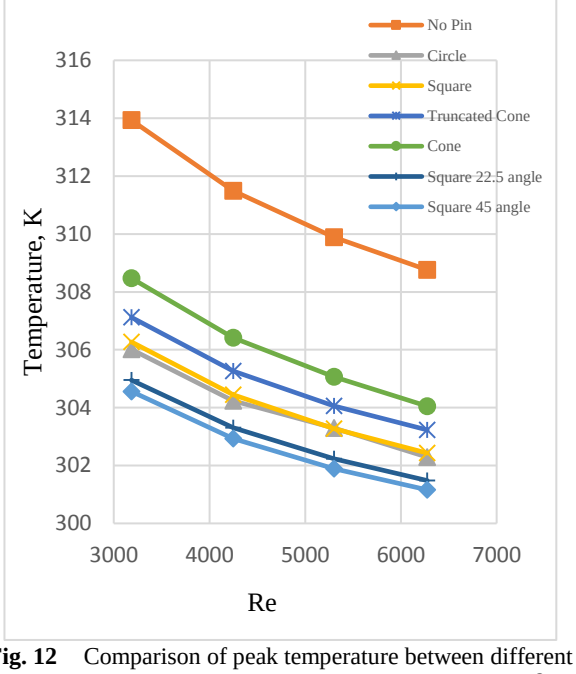

Fig. 12 Comparison of peak temperature between different models of heatsink with thermal heat flux of 0.5 W/cm^2.

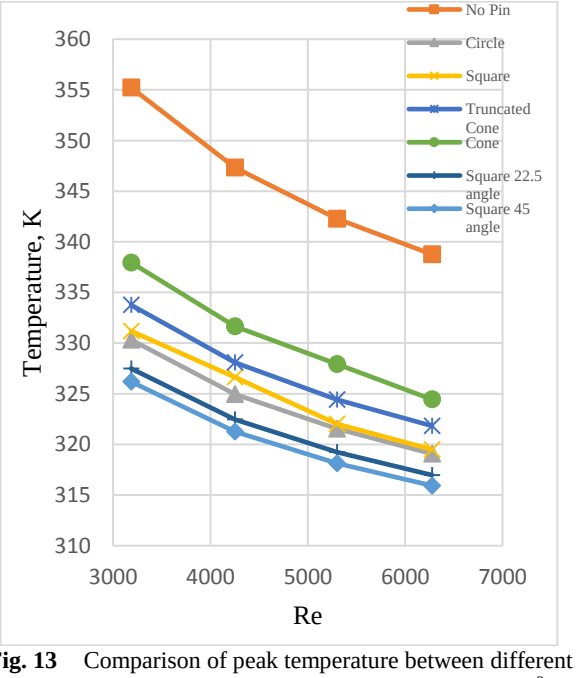

Fig. 13 Comparison of peak temperature between different models of heatsink with thermal heat flux of 1.5 W/cm^2.

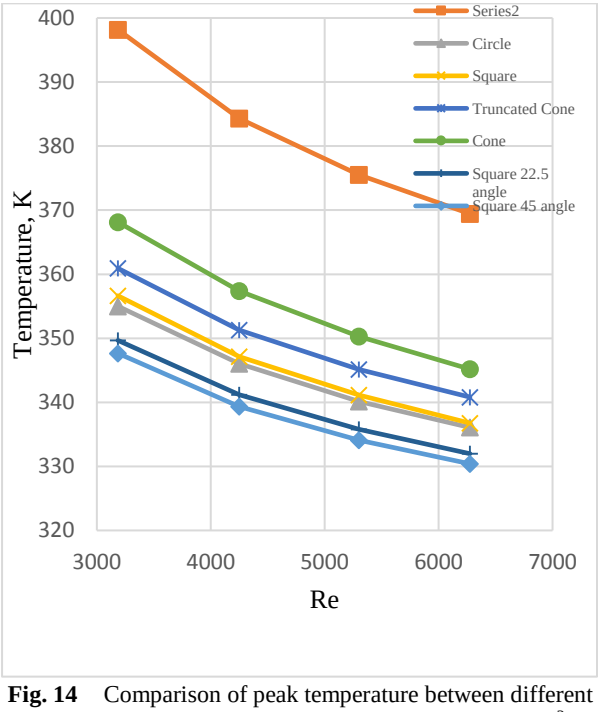

Fig. 14 Comparison of peak temperature between different models of heatsink with thermal heat flux of 2.5 W/cm^2.

The plate-fin heat sink has the highest max temperature out of all of these models, having its highest temperature reaction near 400 Kelvin in one of the experiments. This result shows that even having a simple 3 pin per layer decreases the peak temperature by over 30 degrees in higher heat fluxes. Figures 15, 16 and 17 show the pressure drop between the inlet and outlet of the numerical model. The figures show that the square pin heatsinks have the most pressure drop when compared to the other heatsink models due to their shape and geometry.

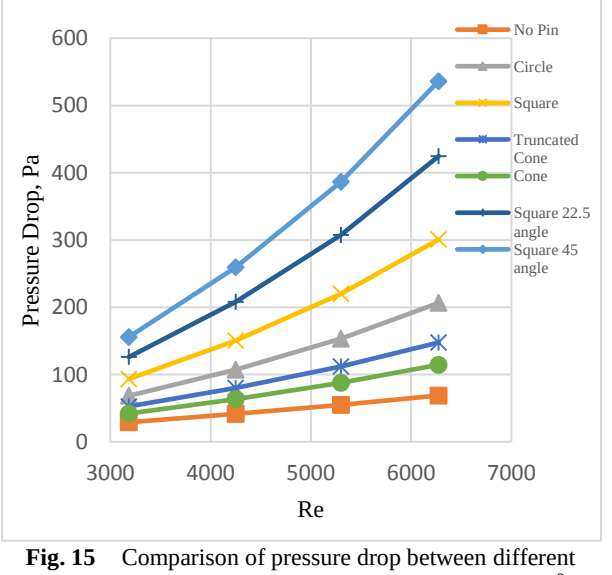

Fig. 15 Comparison of pressure drop between different models of heatsink with thermal heat flux of 0.5 W/cm^2.

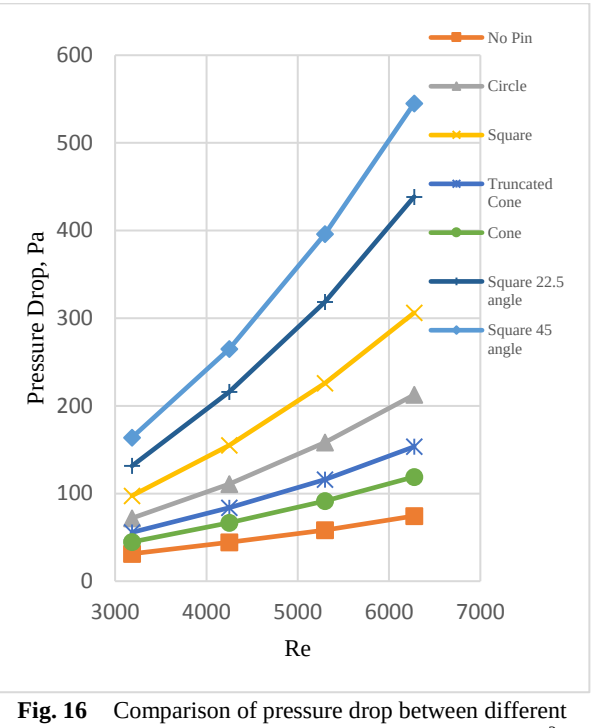

Fig. 16 Comparison of pressure drop between different models of heatsink with thermal heat flux of 1.5 W/cm^2.

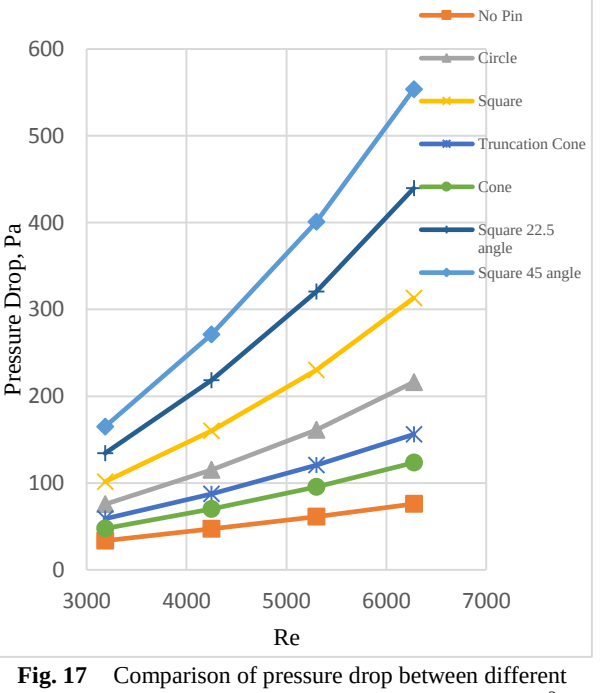

Fig. 17 Comparison of pressure drop between different models of heatsink with thermal heat flux of 2.5 W/cm^2.

It also shows that by tilting the pin in the square model heatsink by 22.5 and 45 degrees, the pressure drops increase by at least 34 percent and 66 percent, respectively. With increasing the coolant airspeed and therefore with the increase of the Reynolds number, the pressure drop difference between the square model with 0-degree angle deflection compared to the circular

model changes between 30% up to 45% with the increase of inlet speed. It can be concluded that despite having nearly the same peak temperature, the amount of energy required for cooling the square pin fin heat sin is about 30 to 45 percent more than the circular pin fin heat sink. The other models are also shown here have less pressure drop due to their shape and geometry not obscuring the airflow between the fins compared to the circular and square shape models of pin fin heatsink. The truncated cone despite having a higher peak temperature consumes up to 27 percent less energy compared to the circular pin model. The cone-shaped pin fin heat sink has the least pressure drop when compared to the other pin-based model heat skinks even though it has a higher peak temperature. The PFHT heatsink has the least pleasure drop due to having no obstruction for the airflow, therefore, uses the least energy comparatively but when comparing the peak temperature, it has the highest of all of the heatsink models.

Figures 18, 19 and 20 show the Nusselt number of each of the models for different Reynolds number with different heat fluxes. Comparing the Nusselt number of these models shows that the Nusselt number of the truncated cone pin fin heat sink is only about 5 percent less than the circular pin fin heat skink while the Nusselt number of the cone-shaped pin heat sink is 10 to 11 percent less than the circular model.

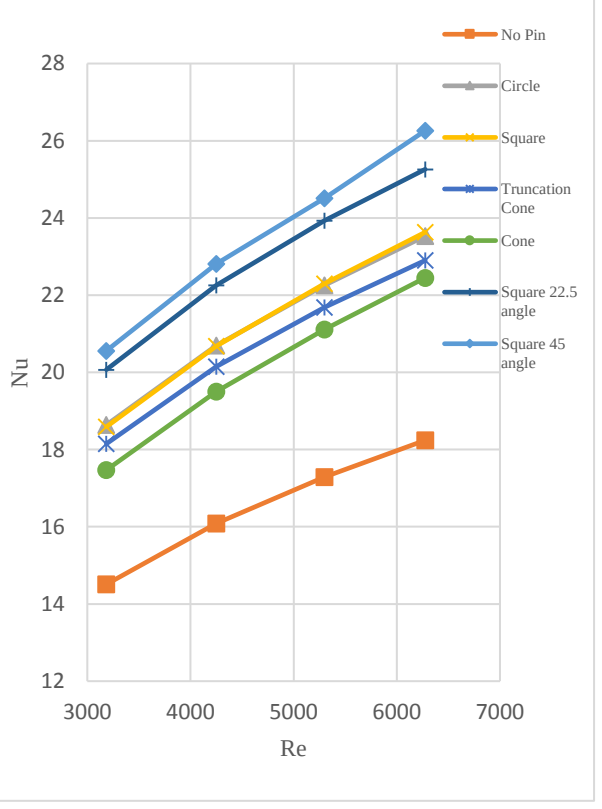

Fig. 18 Comparison of Nusselt number between different models of heatsink with thermal heat flux of 0.5 W/cm^2.

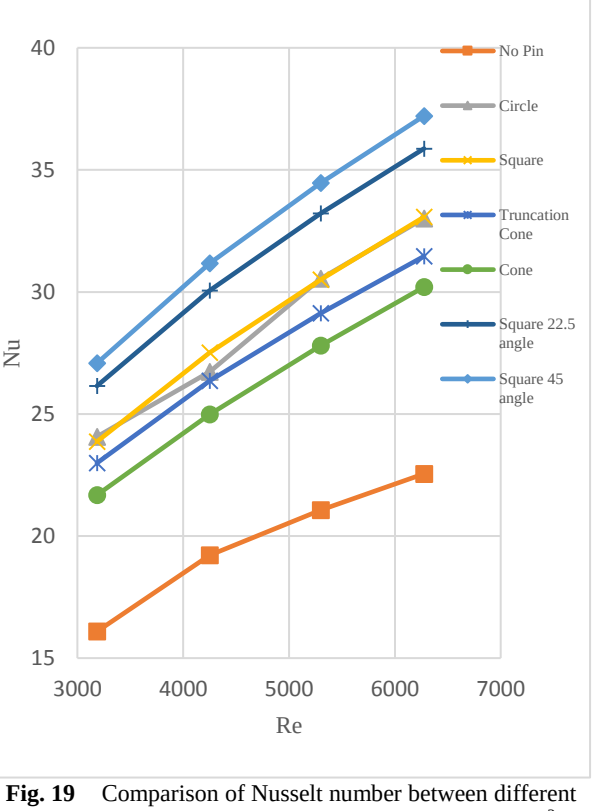

Fig. 19 Comparison of Nusselt number between different models of heatsink with thermal heat flux of 1.5 W/cm^2.

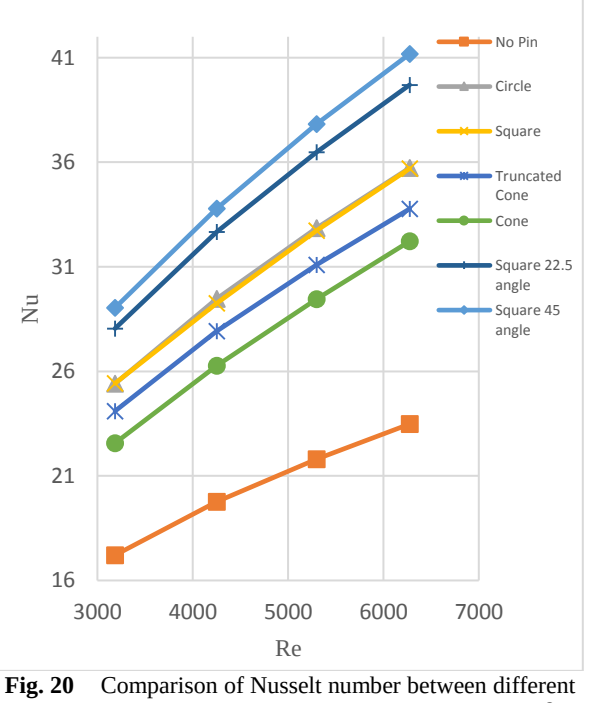

Fig. 20 Comparison of Nusselt number between different models of heatsink with thermal heat flux of 2.5 W/cm^2.

This shows that despite having less Nusselt number, the energy required to cool the heatsinks is significantly less for both of the cone-shaped models. by looking at the

pressure figures, it can also be interpreted that the square shape and the circular shape pin fin heat sink work better in slower air currents. The highest Nusselt number belongs to the square pinned hit sin with a 45-degree deflection angle. This is due to the change of the angle in the square pin and how air contacts more surface area compared to the square pin with no deflection angle which would increase thermal performance. When compared to the circular and the square pin model with no deflection angle, by changing the deflection angle by 22.5 and 45 degrees, the Nusselt number would increase by 7.6 and 11 percent for lower fluxes. In higher fluxes, the difference is increased to 10.3 and 14.2 percent, respectively. Truncated cone pin heat sink when compared to the circle pin heat sink has 2.6 percent up to 5.1 percent less Nusselt number.

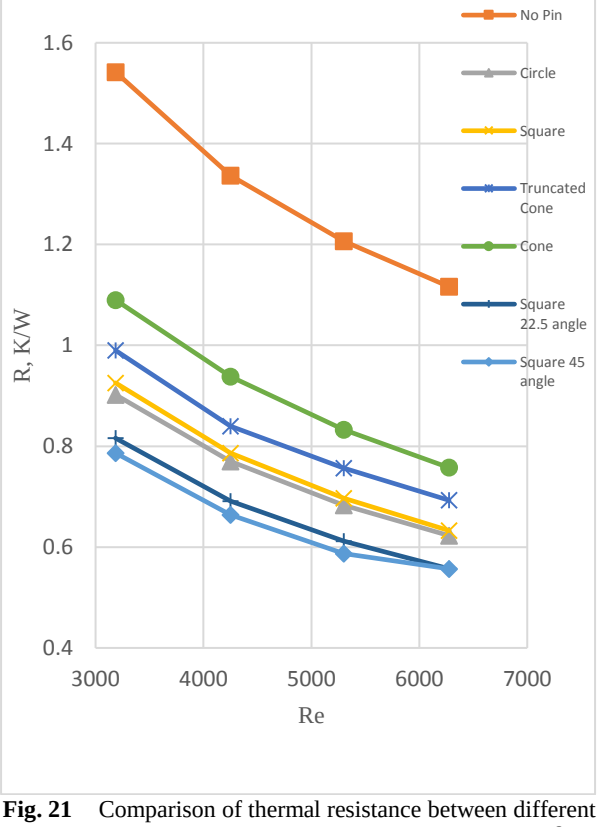

Fig. 21 Comparison of thermal resistance between different models of heatsink with thermal heat flux of 0.5 W/cm^2.

Figures 21, 22 and 23 show the thermal resistance of the models for different Reynolds number and different heat fluxes. The same explanation for the Nusselt number can also be attributed to the thermal resistance of each model. The square pin heat sink model comes on top with having the least thermal heat resistance out of all the heatsink models while the truncated cone and cone pin heatsink models have higher heat resistance due to having higher temperature compared to the models mentioned above.

The thermal performance of the square model heat sink with 22.5- and 45-degrees deflection angle is increased by 9.6 and 12 percent when compared to the circular pin model heat sink.

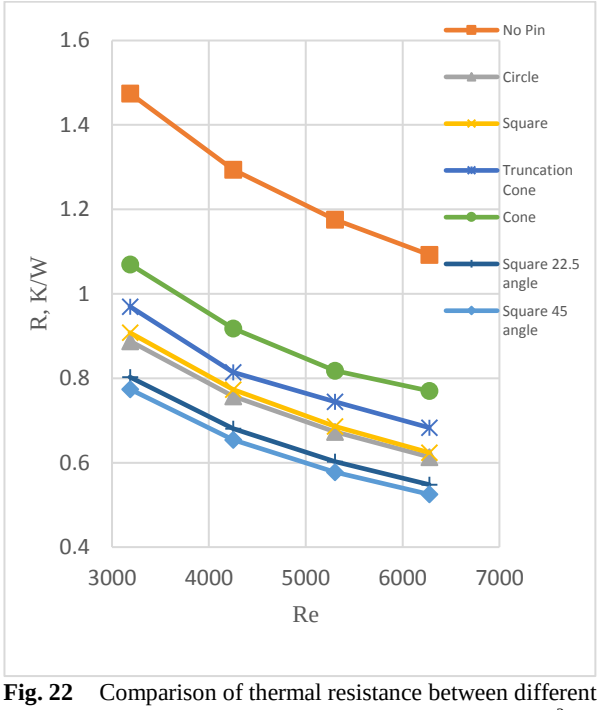

Fig. 22 Comparison of thermal resistance between different models of heatsink with thermal heat flux of 1.5 W/cm^2.

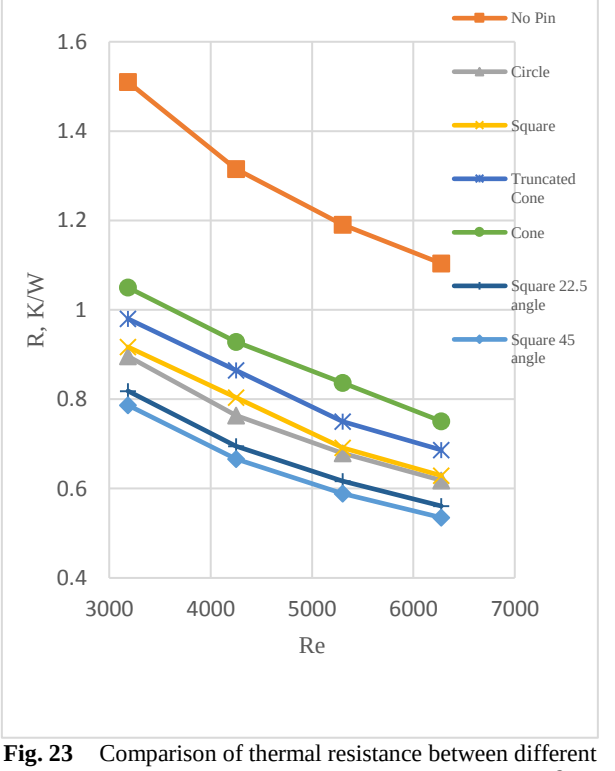

Fig. 23 Comparison of thermal resistance between different models of heatsink with thermal heat flux of 2.5 W/cm^2.

Figures 24, 25, and 26 show the energy consumption for each of these heatsink models. The square-shaped pin heatsink model uses the most energy and the PFHS uses the least amount of energy.

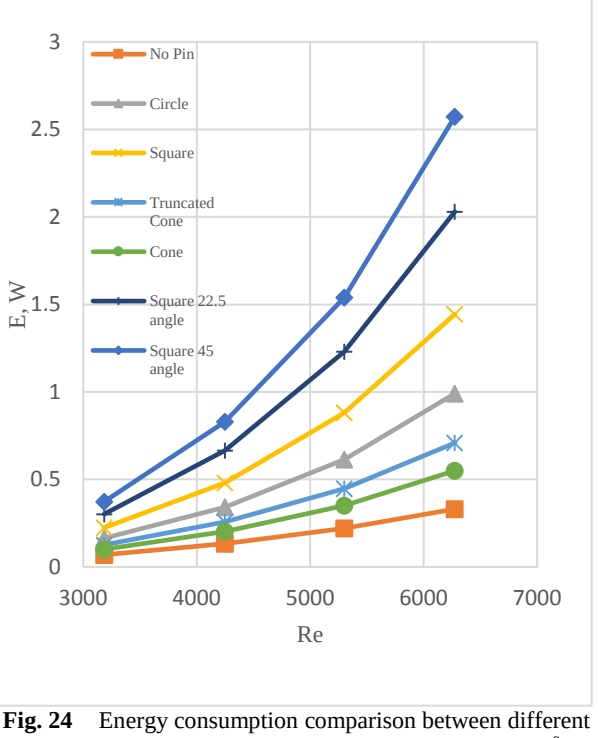

Fig. 24 Energy consumption comparison between different models of heatsink with thermal heat flux of 0.5 W/cm^2.

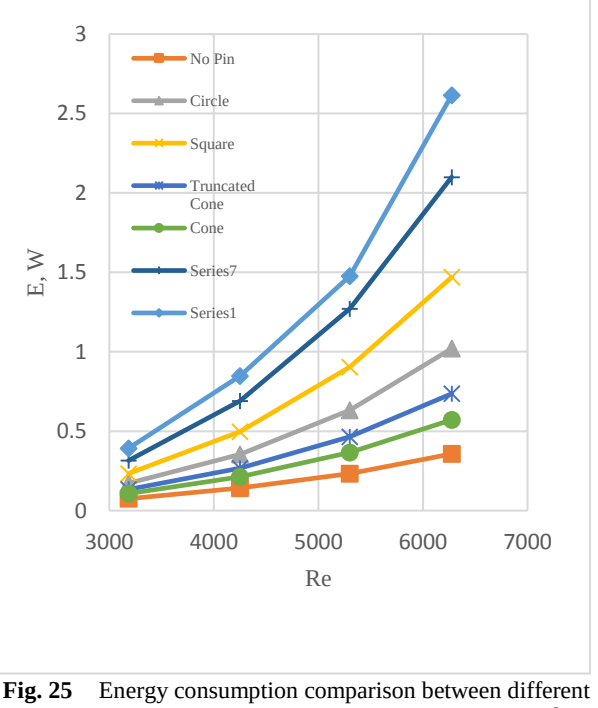

Fig. 25 Energy consumption comparison between different models of heatsink with thermal heat flux of 1.5 W/cm^2.

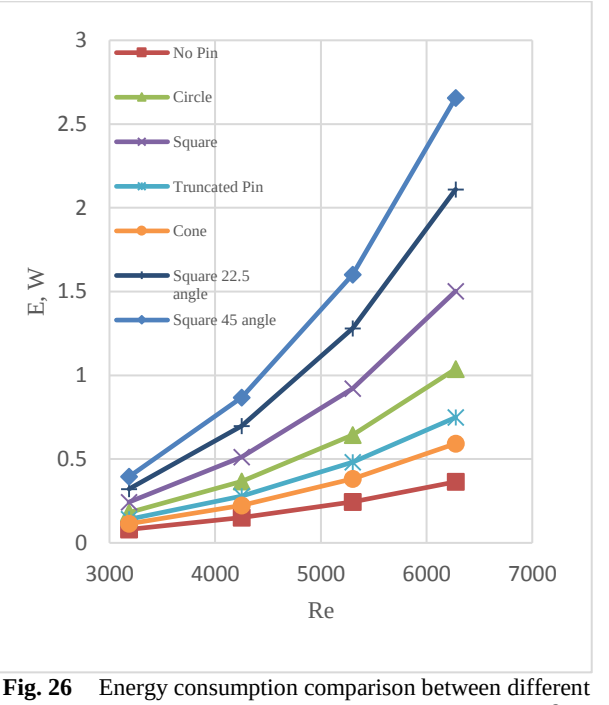

Fig. 26 Energy consumption comparison between different models of heatsink with thermal heat flux of 2.5 W/cm^2.

The geometry and the shape of the pin between the fin in the heatsink have a profound effect on pressure drop that even changing the angle of attack will increase the pressure drop considerably. This correlates to the amount of energy used for cooling these models of heat sinks. Figures 27 to 32 show the thermal contours of the different models of heat sink under the same velocity and heat flux of 8 m/s and 1.5 watts per centimeter square. The air passing through between the fins gets heated up by the fins and the pins. It also shows how are the transfers between the fin and pins and the air by convection. When comparing the circle-shaped pin, the size of the area decreases for the truncated cone and the cone pin model heatsink thereby increasing maximum temperature but reducing pressure drop compared to the regular circle-shaped pin heat sink model. it also shows that by turning the pin in square model heatsinks, it can reduce maximum temperature while increasing pressure drop.

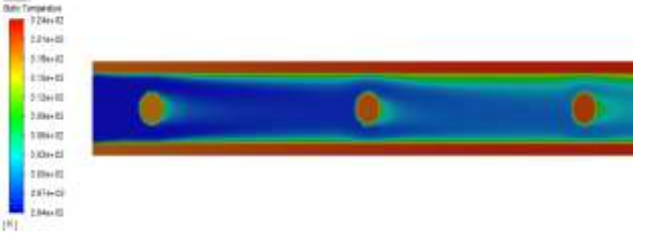

Fig. 27 Temperature contour of Circle Pin Heatsink model with the velocity of 8 m/s with thermal heat flux of 1.5 W/cm.

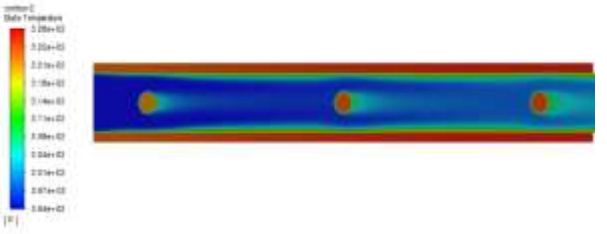

Fig. 28 Temperature contour of truncated cone pin heatsink model with the velocity of 8 m/s with thermal heat flux of 1.5 W/cm^2.

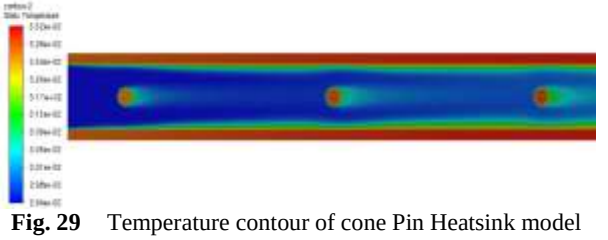

Fig. 29 Temperature contour of cone Pin Heatsink model with the velocity of 8 m/s with thermal heat flux of 1.5 W/cm^2.

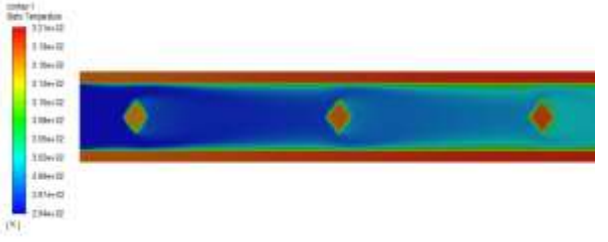

Fig. 30 Temperature contour of 45-degree angle square Pin Heatsink model with the velocity of 8 m/s with thermal heat flux of 1.5 W/cm^2.

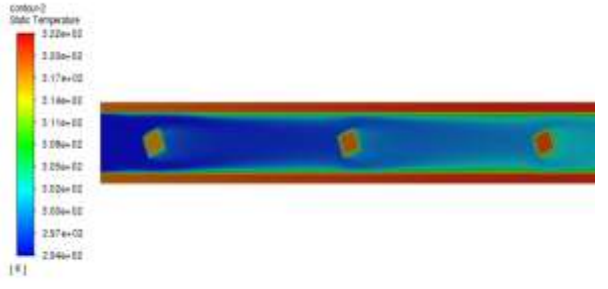

Fig. 31 Temperature contour of 22.5-degree angle square Pin model with the velocity of 8 m/s with thermal heat flux of 1.5 W/cm^2.

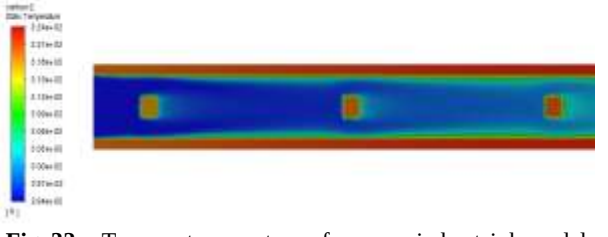

Fig. 32 Temperature contour of square pin heatsink model with the velocity of 8 m/s with thermal heat flux of 1.5 W/cm^2.

Figures 33 to 38 show the velocity of the heat sin models with the velocity of 8m/s. It shows how the air interacts with the pin between the fin in these heatsinks models. Also shows us how the air current moves around the pins. The circle model air current counter is similar to that of a cylinder with the difference that the diameter changes with height change. The square models show how the air staggers when approaching the square pin. This staggering increases by changing the angle of the square pin.

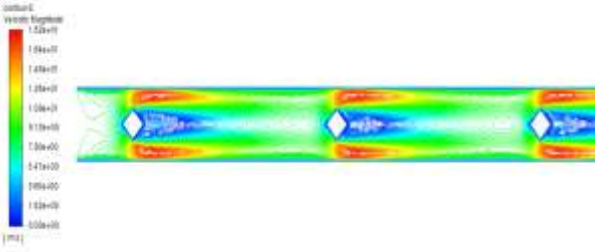

Fig. 33 Velocity contour of 45-degree angle square Pin Heatsink model with the velocity of 8 m/s with thermal heat flux of 1.5 W/cm^2.

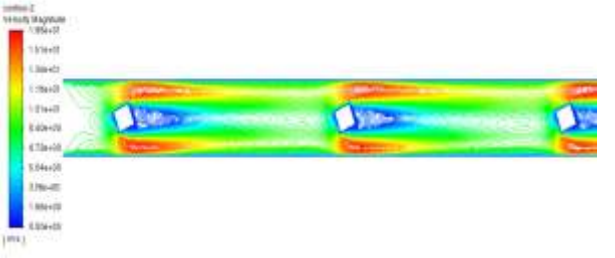

Fig. 34 Velocity contour of 22.5-degree angle square Pin model with the velocity of 8 m/s with thermal heat flux of 1.5 W/cm^2.

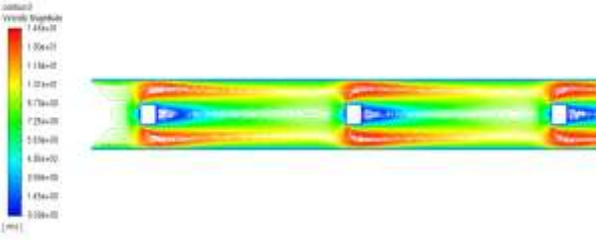

Fig. 35 Velocity contour of square pin heatsink model with the velocity of 8 m/s with thermal heat flux of 1.5 W/cm^2.

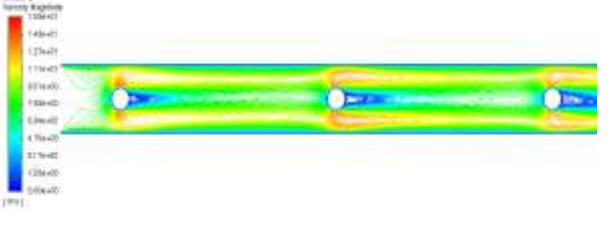

Fig. 36 Velocity contour of truncated cone pin heatsink model with the velocity of 8 m/s with thermal heat flux of 1.5 W/cm^2.

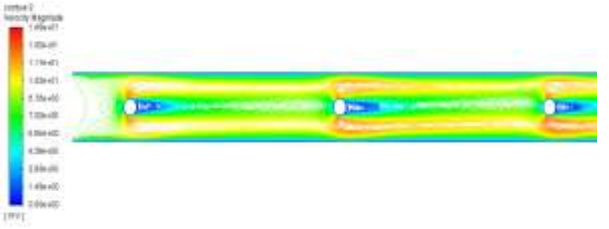

Fig. 37 Velocity contour of cone Pin Heatsink model with the velocity of 8 m/s with thermal heat flux of 1.5 W/cm^2**.**

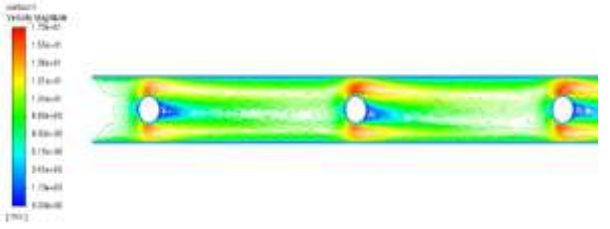

Fig. 38 Velocity contour of Circle Pin Heatsink model with the velocity of 8 m/s with thermal heat flux of 1.5 W/cm^2.

6 CONCLUSIONS

In this Numerical experiment, several models of heatsinks with different pin models (except for the PFHS) were compared in different factors such as peak temperature, heat resistance, thermal performance, and energy consumption. The results are as follows:

1- With the increase of Reynolds, number increases flow resistance and therefore it will increase the pressure drop in each model of the heatsink. The square pin has the most pressure drop out of all of these models due to its geometry therefore it consumes the most energy when compared to the other models.

2- By changing the angle of attack, the pressure drop for the square pin heatsink increased due to more air hitting the pins. This increase for 22.5 and 45 angles of deflection is measured to be at least more than 34 and 66 percent compared to the square pin heatsink model with zero angles of deflection.

3- The cone-shaped pin fin heat sink model has less Nusselt number compared to the rest of the models but consumes the least amount of energy for cooling. Therefore, it is far more economical to use these models at higher velocity compared to the other models of heatsinks.

4- The PFHS has the least pressure drop due to having no pin in front of the air current making it ideal for certain heat sink designs. It has the highest thermal resistance and the lowest Nusselt number compared to the rest of the models. It also shows that adding a simple 3 pins for each layer of the heatsink thermal performance by at least 28 percent.

5- The truncated cone and cone model show us that changing the model's geometry can help us reduce pressure drop with the sacrifice of little thermal performance.

6- Changing the angle of deflection for the square by 22.5 and 45 degrees increases the thermal performance of the square pin heat sink by at least 9.6 and 12 percent respectively compared to the regular square pin heat sink model.

7 APPENDIX OR NOMENCLATURE

Nomenclature	Greek symbols
Latin Symbols	P Dimensionless pressure
A Areas [m^2]	σ Constant In the turbulent model
C Constant in turbulent model	δ Fin spacing [mm]
H Height [m]	Δ Differential
L Distance from base In x-direction [m]	μ Viscosity [$N.s/m^2$]
N Fin number [-]	ρ Density [$kg.m^{-3}$]
p Pressure [Pa]	θ Dimensionless temperature
E Pumping power [W]	Subscripts
Q Heating power [W]	i, j Repeated-subscript indices
R Resistance [$K.W^{-1}$]	in Inlet
Re Reynolds number [-]	t Turbulent Flow
T Temperature [K]	out Outlet
x, y, z Cartesian coordinates	th Thermal
X, Y, Z Dimensionless Cartesian Coordinates	p Flow passage
U, V, W Dimensionless velocity	s Solid
D_H Hydraulic diameter	w Wall
Nu Nusselt Number	f Fluid

REFERENCES

[1] Hosseini, S. M., Safaei, M. R., Goodarzi, M., Alrashed, A. A. A. A., and Nguyen, T. K., New Temperature, Interfacial Shell Dependent Dimensionless Model for Thermal Conductivity of Nanofluids, International Journal of Heat and Mass Transfer, Vol. 114, 2017, pp. 207-210, https://doi.org/10.1016/j.ijheatmasstransfer.2017.06.061

[2] Talebi, M., Tabibian, M., Magnetic Field Effect on Ferro-Nanofluid Heat Transfer in a Shell and Tube Heat Exchanger with Seven Twisted Oval Tubes, ADMT Journal, Vol. 15, No. 2, 2022, pp. 39-48, 10.30495/admt.2022.1937049.1300.

[3] Kurşun, B., Sivrioğlu, M., Heat Transfer Enhancement Using U-Shaped Flow Routing Plates in Cooling Printed Circuit Boards, Journal of the Brazilian Society of Mechanical Sciences and Engineering, Vol. 40, No. 1, 2018, pp. 1-14.

[4] Ghasemi, S. E., Ranjbar, A. A., and Hosseini, M. J., Experimental Evaluation of Cooling Performance of Circular Heat Sinks for Heat Dissipation from Electronic Chips Using Nanofluid, Mechanics Research Communications, Vol. 84, 2017, pp. 85-89,https://doi.org/10.1016/j.mechrescom.2017.06.009.

[5] Sadeghi, H., Izadpanah, E., Babaie Rabiee, M., and Hekmat, M. H., Effect of Cylinder Geometry on The Heat Transfer Enhancement of Power-Law Fluid Flow Inside a Channel, Journal of the Brazilian Society of Mechanical Sciences and Engineering, Vol. 39, No. 5, 2017, pp. 1695-1707, 10.1007/s40430-016-0695-3.

[6] Ghani, I. A., Kamaruzaman, N., and Sidik, N. A. C., Heat Transfer Augmentation in A Microchannel Heat Sink with Sinusoidal Cavities And Rectangular Ribs, International Journal of Heat and Mass Transfer, Vol. 108, 2017, pp. 1969-1981, https://doi.org/10.1016/j.ijheatmasstransfer.2017.01.046.

[7] Mousavi, H., Rabienataj Darzi, A. A., Farhadi, M., and Omidi, M., A Novel Heat Sink Design with Interrupted, Staggered and Capped Fins, International Journal of Thermal Sciences, Vol. 127, 2018, pp. 312-320, https://doi.org/10.1016/j.ijthermalsci.2018.02.003.

[8] Jajja, S. A., Ali, W., Ali, H. M., and Ali, A. M., Water Cooled Minichannel Heat Sinks for Microprocessor Cooling: Effect of Fin Spacing, Applied Thermal Engineering, Vol. 64, No. 1, 2014, pp. 76-82, https://doi.org/10.1016/j.applthermaleng.2013.12.007.

[9] Patel, N., Mehta, H. B., Experimental Investigations on A Variable Channel width Double Layered Minichannel Heat Sink, International Journal of Heat and Mass Transfer, Vol. 165, 2021, pp. 120633, https://doi.org/10.1016/j.ijheatmasstransfer.2020.120633.

[10] Abbasian Arani, A. A., Akbari, O., Safaei, M. R., Marzban, A., Alrashed, A., Ahmadi, G., and Nguyen, T., Heat Transfer Improvement of Water/Single-Wall Carbon Nanotubes (SWCNT) Nanofluid in A Novel Design of a Truncated Double-Layered Microchannel Heat Sink, International Journal of Heat and Mass Transfer, Vol. 113, 2017, pp. 780-795, 10.1016/j.ijheatmasstransfer.2017.05.089.

[11] Engerer, J. D., Doty, J. H., and Fisher, T. S., Transient Thermal Analysis of Flash-Boiling Cooling in the Presence of High-Heat-Flux Loads, International Journal of Heat and Mass Transfer, Vol. 123, 2018, pp. 678-692, https://doi.org/10.1016/j.ijheatmasstransfer.2018.02.109.

[12] Al-damook, A., Alkasmoul, F., Heat Transfer and Airflow Characteristics Enhancement of Compact Plate-Pin Fins Heat Sinks-A Review, Propulsion and Power Research, Vol. 7, No. 2, 2018, pp. 138-146, https://doi.org/10.1016/j.jppr.2018.05.003.

[13] Yang, Y. T., Peng, H. S., Investigation of Planted Pin Fins for Heat Transfer Enhancement in Plate Fin Heat Sink, Microelectronics Reliability, Vol. 49, No. 2, 2009, pp. 163-169, https://doi.org/10.1016/j.microrel.2008.11.011.

[14] Li, H. Y., Chao, S. M., Measurement of Performance of Plate-Fin Heat Sinks with Cross Flow Cooling, International Journal of Heat and Mass Transfer, Vol. 52, No. 13, 2009, pp. 2949-2955, https://doi.org/10.1016/j.ijheatmasstransfer.2009.02.025.

[15] Alam, M. W., Bhattacharyya, S., Souayeh, B., Dey, K., Hammami, F., Rahimi-Gorji, M., and Biswas, R., CPU Heat Sink Cooling by Triangular Shape Micro-Pin-Fin: Numerical Study, International Communications in Heat and Mass Transfer, Vol. 112, 2020, pp. 104455, https://doi.org/10.1016/j.icheatmasstransfer.2019.104455.

[16] Haghighi, S. S., Goshayeshi, H. R., and Safaei, M. R., Natural Convection Heat Transfer Enhancement in New Designs of Plate-Fin Based Heat Sinks, International Journal of Heat and Mass Transfer, Vol. 125, 2018, pp. 640-647, https://doi.org/10.1016/j.ijheatmasstransfer.2018.04.122.

[17] Ahmed, H. E., Salman, B. H., Kherbeet, A. S., and Ahmed, M. I., Optimization of Thermal Design of Heat Sinks: A Review, International Journal of Heat and Mass Transfer, Vol. 118, 2018, pp. 129-153, https://doi.org/10.1016/j.ijheatmasstransfer.2017.10.099.

[18] Kim, S. J., Kim, D. K., and Oh, H. H., Comparison of Fluid Flow and Thermal Characteristics of Plate-Fin and Pin-Fin Heat Sinks Subject to a Parallel Flow, Heat Transfer Engineering, Vol. 29, No. 2, 2008, pp. 169-177, 10.1080/01457630701686669.

[19] Ambreen, T., Kim, M.-H., Flow and Heat Transfer Characteristics Over a Square Cylinder with Corner Modifications, International Journal of Heat and Mass Transfer, Vol. 117, 2018, pp. 50-57, https://doi.org/10.1016/j.ijheatmasstransfer.2017.09.132.

[20] Scholten, J. W., Murray, D. B., Unsteady Heat Transfer and Velocity of a Cylinder in Cross Flow—I. Low Freestream Turbulence, International Journal of Heat and Mass Transfer, Vol. 41, No. 10, 1998, pp. 1139-1148, https://doi.org/10.1016/S0017-9310(97)00250-0.

[21] Bhattacharyya, S., Das, S., Sarkar, A., Guin, A., and Mullick, A., Numerical Simulation of Flow and Heat Transfer Around Hexagonal Cylinder, International Journal of Heat and Technology, Vol. 35, No. 2, 2017, pp. 360-363.

[22] Benim, A. C., Pasqualotto, E., and Suh, S. H., Modelling Turbulent Flow Past a Circular Cylinder by RANS, URANS, LES and DES, Progress in Computational Fluid Dynamics, An International Journal, Vol. 8, No. 5, 2008, pp. 299-307.

[23] Nilpueng, K., Mesgarpour, M., Asirvatham, L. G., Dalkılıç, A. S., Ahn, H. S., Mahian, O., and Wongwises,

S., Effect of Pin Fin Configuration on Thermal Performance of Plate Pin Fin Heat Sinks, Case Studies in Thermal Engineering, Vol. 27, 2021, pp. 101269.

[24] Nilpueng, K., Wongwises, S., Thermal Performance Investigation of a Plate Fin Heat Sink Equipped with Twisted Tape and Perforated Twisted Tape, Journal of Thermal Science and Technology, Vol. 16, No. 2, 2021, pp. JTST0024-JTST0024, 10.1299/jtst.2021jtst0024.

[25] Sertkaya, A. A., Ozdemir, M., and Canli, E., Effects of Pin Fin Height, Spacing and Orientation to Natural Convection Heat Transfer for Inline Pin Fin and Plate Heat Sinks by Experimental Investigation, International Journal of Heat and Mass Transfer, Vol. 177, 2021, pp. 121527, https://doi.org/10.1016/j.ijheatmasstransfer.2021.121527.

[26] El-Said, E. M. S., Abdelaziz, G. B., Sharshir, S. W., Elsheikh, A. H., and Elsaid, A. M., Experimental Investigation of The Twist Angle Effects on Thermo-Hydraulic Performance of a Square and Hexagonal Pin Fin Array in Forced Convection, International Communications in Heat and Mass Transfer, Vol. 126, 2021, pp. 105374, https://doi.org/10.1016/j.icheatmasstransfer.2021.105374.

[27] Singh, N. R., Onkar, S., and Ramkumar, J., Thermo-Hydraulic Performance of Square Micro Pin Fins under Forced Convection, Journal homepage: http://iieta. org/journals/ijht, Vol. 39, No. 1, 2021, pp. 170-178.

[28] Mate, D. M., Tale, V. T., Effects of Pin Fin Arrangement Its Heat Transfer Characteristics on Performance of Heat Sink, Materials Today: Proceedings, Vol. 43, 2021, pp. 2377-2382.

[29] Davoudi, A., Daneshmand, S., Monfared, V., and Mohammadzadeh, K., Numerical Simulation on Heat Transfer of Nanofluid in Conical Spiral Heat Exchanger, Progress in Computational Fluid Dynamics, an International Journal, Vol. 21, No. 1, 2021, pp. 52-63.

[30] Yuan, W., Zhao, J., Tso, C. P., Wu, T., Liu, W., and Ming, T., Numerical Simulation of the Thermal Hydraulic Performance of a Plate Pin Fin Heat Sink, Applied Thermal Engineering, Vol. 48, 2012, pp. 81-88, 10.1016/j.applthermaleng.2012.04.029.

[31] Li, H. Y., Chen, K. Y., and Chiang, M. H., Thermal-Fluid Characteristics of Plate-Fin Heat Sinks Cooled by Impingement Jet, Energy Conversion and Management, Vol. 50, No. 11, 2009, pp. 2738-2746, https://doi.org/10.1016/j.enconman.2009.06.030.

[32] Sparrow, E. M., Ramsey, J. W., and Altemani, C. A. C., Experiments on In-Line Pin Fin Arrays and Performance Comparisons with Staggered Arrays, 1980.

[33] Yu, X., Feng, J., Feng, Q., and Wang, Q., Development of a Plate-Pin Fin Heat Sink and Its Performance Comparisons with A Plate Fin Heat Sink, Applied Thermal Engineering, Vol. 25, No. 2, 2005, pp. 173-182, https://doi.org/10.1016/j.applthermaleng.2004.06.016.